OPEN ACCESS

Kashf Journal of Multidisciplinary Research
Vol: 03 - Issue 04 (2026)
P-ISSN: 3007-1992 E-ISSN: 3007-200X
https://kjmr.com.pk

MANGANESE FERRITE NANOPARTICLES FOR ENHANCED REMOVAL OF ORGANIC CONTAMINANTS FROM WATER

Muhammad Arslan[1], Hafiz Safdar Ali[2], Aqsa Saleem[3], *Kanwal Akhtar[4], Ayesha Younus[5], Yasir Javed[6]

[1, 2, 3]Faculty of Sciences, The Superior University, Lahore, Pakistan.
[4, 5]Department of Physics, Government College Women University, Faisalabad, Pakistan.
[6]Department of Physics, University of Agriculture, Faisalabad, Pakistan.

***Corresponding Author:** (kanwalakhtar@gcwuf.edu.pk)*

***DOI:**(https://doi.org/10.71146/kjmr891)*

Article Info

Abstract

Manganese ferrite nanoparticles have become very successful nanomaterials for the development of sustainable water purification technologies. With their exact physical and chemical applications such as high surface area, adjustable magnetic behavior, and catalytic activity generated with chemical strength they are capable candidates for complete removal of a range of waste in water covering heavy metals, dyes, pharmaceuticals, and pathogenic microorganisms. Its well-defined spinal framework increases fast intake capacity and makes easier m so that the operative magnetic exclusion charges are lowered, and secondary pollution is lowered during processing. More recently, the progress of synthesis methods including co-precipitation, sol-gel, hydrothermal and green preparation method have directed start-up particle size, shapes and surface treatment. Surface upgrade through polymers, carbon-based materials, or bio-inspired donor molecule further changes selectivity, adsorption efficiency, and reusability. In specific, manganese ferrite nanoparticles showing strong output in advanced oxidation processes , where they run as heterogeneous catalysts in Fenton-like reactions to give rise to reactive products oxygen species flexible of breaking down resistant organic pollutants. From a sustainability outlook, manganese ferrites nanoparticles offer many benefits over standard therapy technologies. Their magnetic restorability activated the common reuse without important loss of activity, thereby reduce material waste and treatment costs. Furthermore, the potential of green synthesis using plant division and low-impact precursor swaps with global natural goals and reduce toxic by-products during production. No matter of their helpful potential, issues remain as regards large-scale application, long-term natural impact, nanoparticle balance in complex water matrices, and likely pollution-causing effects. Upgrading biocompatibility, increasing restoring efficiency, and including manganese ferrite nanoparticles bring together treatment systems like membrane filtration, photocatalysis, and adsorption–catalysis connecting processes are the important areas of in progress research. All things driven, manganese ferrite nanoparticles offer an elastic and environment-friendly selection for water purifying systems of the future. Their high draw efficiency, catalytic flexibility, and magnetic make them ease of separation important materials for flagship the world's problems with water shortage and pollution. Continues creativity in material design, green synthesis, and ecological safety analysis will be important for converting laboratory-scale success into real-world water treatment applications.

Keywords: *Manganese ferrite nanoparticles, water purification, sustainable nanotechnology, magnetic separation, adsorption, degradation, Nano catalysis, recyclability.*

Introduction

The control and manipulation of materials at the nanoscale, usually between 1 and 100 nanometers, where matter exhibits properties different from those at the bulk scale, is the focus of the quickly developing discipline of nanotechnology [1]. While nanosized particles have existed and interacted with humans for generations, scientific research began in the early 1900s when Richard Zsigmondy created the nanometer as a unit for particle measurement and successfully detected nanoscale materials. Richard Feynman's seminal 1959 speech, which stressed the prospect of directing matter at the atomic level, laid the theoretical foundation for modern nanotechnology [2]. Norio Taniguchi helped to codify this idea by referring to atom-scale production in industrial processes as "nanotechnology." Important scientific accomplishments in the 1980s, such as the discovery of fullerenes, the idea of molecular nanotechnology by Eric Drexler, and the production of carbon nanotubes by Sumio Iijima, considerably increased the scope of the area [3]. At the initiate of the 21st century, nanotechnology became a systematic research priority, specifically in the United States [4]. This commitment was conditioned by the enactment of the 21st Century Nanotechnology Research and Development Act, which constructed the National Nanotechnology Initiative (NNI). The NNI and its Nano-scale science technology subcommittee are in capacity of NNI coordination, including study design, funding, and cross-agency association. Through this mixed national framework, nanotechnology research has increasing speed and managed to key progress across different industries like as healthcare, electronics, energy systems, and environmental protection [5]

Nanomaterials are stated by their property scale at the nanoscale, commonly around 10^{-9} m. Material action is guided by surface and boundary-related events rather than macroscopic properties. Standard boundaries between physics, chemistry, mechanics, and materials science become unclear. This union is the foundation of nanoscience and sustains the speedy progress of nanomaterials research, which has been clarified by improved experimental techniques for nanoscale review and control, as well as critical approaches created for small length and time scales [6]. Understanding length scales from atomic radii and crystal lattice partition at the atomic scale level to nanoscale layout like DNA and carbon nanotubes, and active on to viruses, metallic grains, bacteria, and biotic cells at the micro and macroscales, is important for a thorough efficiency of nanomaterials. This proceeds categorization of scales places nanoparticles in both natural and artificial systems, basic their invisible scientific significance and technological applicability [7]

The categorization of nanomaterials dependent on number of dimensions—the number of dimensions that decrease within the nano-meter scale range—is important to absorbing the connections in between their structure and properties. All three dimensions are confined within the nanoscale in zero-dimensional (0D) nanomaterials, which include semiconductor quantum dots like CdSe and gold and silver nanoparticles. These materials have dimensional optical and electronic characteristics [6]. Carbon nanotubes, nanowires, and nanorods—such as silicon and ZnO nanorods—are basic examples of one-dimensional (1D) nanomaterials, which have two dimensions at the nanoscale and a third dimension that expand beyond it to produce anisotropic properties. These materials are used widely in sensors and electronic devices. High surface area and distinct mechanical and electrical behavior are characteristics of two-dimensional (2D) nanomaterials, which only have one dimension in the nanoscale range.

Graphene, transition metal dichalcogenide nanosheets like MoS_2, and layered oxide nanosheets are notable examples [9]. Three-dimensional (3D) nanomaterials are made up of nanoscale building blocks assembled

into bulk structures; examples include nanocomposites, nanoporous materials, and aerogels, such as polymer-clay nanocomposites and mesoporous silica.

Diamagnetic materials slight negative magnetic susceptibility is a reflection of the extremely weak magnetization seen in diamagnetic materials, which resists an applied magnetic field. When an external magnetic field is applied, an induced magnetic moment is created in the opposite direction of the field because all electrons are coupled and do not produce a permanent magnetic moment. In reality, diamagnetism is a universal phenomenon seen in all materials, but it only becomes noticeable in the absence of stronger magnetic effects (ferromagnetic or paramagnetic). Copper, gold, bismuth, silicon, and water are common examples of diamagnetic materials, and their susceptibility is virtually temperature independent [10]

Paramagnetic materials possess one or more unpaired electrons in their atoms or ions, which results in persistent magnetic dipole moments that are not significantly interacting with one another. There is no net magnetization when there is no external field present because these moments are oriented randomly. A weak net positive magnetization that is precisely proportional to the strength of the external magnetic field is created when the magnetic moments partially align with the field. According to Curie's law, the paramagnetic susceptibility is tiny and usually diminishes as the temperature rises. Magnesium, platinum, aluminum, and several transition metal ion complexes are a few examples [11].

Ferromagnetic materials exhibit significant magnetic ordering even in the absence of an external field because atomic magnetic moments cooperatively align in the same direction. These materials can maintain their magnetization even after the applied field is removed because of the significant positive magnetic susceptibility, spontaneous magnetization, and magnetic hysteresis caused by this long-range ordering. Above a specific Curie temperature, the material turns paramagnetic, and the magnetic order collapses. Permanent magnets, transformers, and electromagnetic devices are based on classic ferromagnetic materials, which include iron, cobalt, nickel, and certain alloys [12].

Antiferromagnetic materials are defined by an ordered configuration where adjacent atomic magnetic moments align with identical amplitude in antiparallel orientations, producing zero macroscopic net magnetization. Exchange interactions give birth to this antiparallel ordering, which is stable below a Néel temperature particular to the material. Above this temperature, thermal agitation breaks the order and causes the material to behave in a paramagnetic manner. Because of their unique magnetic responses, antiferromagnetic materials—such as manganese oxide (MnO), nickel oxide (NiO), and hematite (α-FeO_3)—are frequently explored in disciplines like spintronics [13].

Ferrimagnetic materials similarly to antiferromagnetic materials, show antiparallel alignment of magnetic moments; but the opposing moment magnitudes are not equal, resulting in a non-zero net magnetization. Magnetite (FeO_4) and other ferrites are examples of mixed-metal oxide compounds with complicated crystal structures that exhibit ferrimagnetism, which is the retention of net magnetization below the Curie temperature. Ferrimagnetic materials are useful in magnetic recording, microwave devices, and biological applications because they combine structural complexity with ferromagnetic order characteristics [14].

Experimental protocol

Chemicals: Manganese nitrate tetrahydrate ($Mn(NO_3)_2{\cdot}4H_2O$), ferric nitrate nonahydrate ($Fe(NO_3)_3{\cdot}9H_2O$), deionized water, sodium hydroxide (NaOH), Polyethylene Glycol, Cellulose were used as precursors in the preparation of $MnFe_2O_4$.

Manganese ferrite nanoparticles ($MnFe_2O_4$) were synthesized using a simple and cost-effective co-precipitation method suitable for sustainable applications in water purification. Analytical-grade ferric chloride hexahydrate ($FeCl_3 \cdot 6H_2O$) and manganese chloride tetrahydrate ($MnCl_2 \cdot 4H_2O$) were used as precursor salts. Initially, appropriate molar amounts of Fe^{3+} and Mn^{2+} salts were dissolved in 100 mL of deionized water under continuous magnetic stirring to maintain a stoichiometric ratio of 2:1. The outcome was heated to around 80°C while stirring to keep complete collapse and homogeneous mixing of metal ions. To start precipitation, 2 M sodium hydroxide (NaOH) solution was fixed slowly until the pH reached 10–11. A dark brown precipitate made at once, showing the making of manganese ferrite nanoparticles. The response mixture was saved at 80°C with carries on stirring for about 2 hours to improved complete initiation and growth of nanoparticles. The engage was then approved to age for 12 hours to improve crystal order and magnetic properties. After attaining of the reaction, the nanoparticles were removing using an outer magnet, which gives their magnetic response and eases renewal for sustainable reuse. The collected precipitate was washed several times with purified water and ethanol to remove inert ions and pollutants. The refined nanoparticles were evaporated in a hot air oven at 80°C for 6 hours and a bit ground into fine powder for growing analysis. As illustrated in figure 1, which presents a flowchart summarizing of FTIR analysis process.

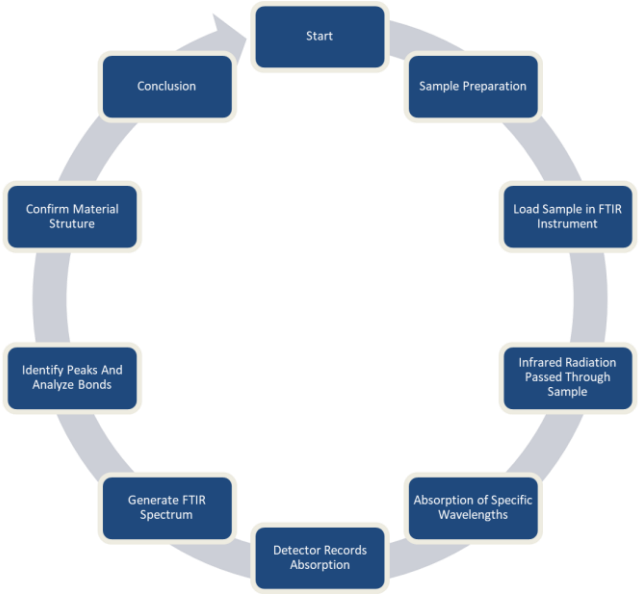

Figure 1: Flowchart Overview: FTIR Spectroscopy Analysis Process

Co-precipitation is a simple method for generating ferrite nanoparticles due to its clarity, low cost, and ability to precisely control particle size. This method requires first dissolving water-soluble salts of the targeted metal ions (such as manganese and iron) in deionized water to extracting a homogeneous solution. Then, an alkaline solution (typically sodium hydroxide or ammonium hydroxide) is progressively added to raise the pH. This pH change enhancing the precipitation of the metal ions as hydroxides. Continuous stirring and moderate heating facilitate the reaction and enhancing the formation of homogeneous nanoparticle nuclei.

To reduce accumulation and direct particle growth, stabilizers such as citric acid or polyethylene glycol can be included. The result precipitate is then obtained, fully washed to remove inert salts and other

pollutants, and dried at an average temperature. As shown in figure 2, the arrangements and analysis of the sample.

Figure 2: Experimental Setup and Sample Procedure of Manganese Ferrites

Definitively, the evaporated material is adjusted at high temperature to change the hydroxide phase into crystalline ferrite nanoparticles with a separate spine structure. In framework, this way helps for correct control over particle size, composition, and shape, making it mainly perfect for the planning of nanomaterials for water treatment, chemical catalysis, and magnetic uses [15].

Characterization

Characterization of the prepared nanoparticles was made using estimate analytical techniques. Fourier transform infrared spectroscopy the presence confirmed of metal–oxygen bonds uses of ferrite materials, while vibrating sample magnetic field analysis was used to calculate magnetic properties, which are important for productive post-treatment separation. It gives details about material bonding, molecular structure, functional groups, and surface chemical properties. This study used FTIR to examine the formation of metal oxygen bonds (or other phase bonds) in nanomaterials, discover surface collector and functional groups, and confirm the structure and formation of co-deposition-fabricated materials. Exceptionally in nanomaterials, FTIR can discover surface hydroxyl groups, adsorbent types, end coating factors, and defects—all of which determine the physicochemical and electrochemical attributes of the material. Recent analysis articles highlight the expanding importance of FTIR in characterizing inorganic materials and nanostructures. [18].

Results and Discussions

The Fourier Transform Infrared (FTIR) spectrum of pure magnesium ferrite ($MgFe_2O_4$) nanoparticles was registered in the range of 4000–900 cm^{-1} to examine the functional groups and verify the formation of the spinel ferrite structure. The acquired spectrum illustrates several characteristic absorption bands reciprocal

to hydroxyl groups, residual organic species, and most importantly, metal–oxygen (M–O) vibrations interlinked with the spinel lattice.

A weak but visible range band shows at approximately 3741 cm^{-1}, given to the improving shaking of free hydroxyl (–OH) groups. This peak refers to fixed on surface moisture or surface hydroxyl groups, regularly created in ferrite nanoparticles due to their high surface-to-volume ratio. Another costly uptake features center-aligned around 3109 cm^{-1} align with hydrogen-bonded O–H pulling vibrations, proposing the presence of physically blended water molecules or surplus hydroxyl groups from primary salts used during synthesis. The enlarged nature of the band confirms hydrogen bonding links, typical in metal oxide nanoparticles began through wet chemical channels such as co-precipitation or sol–gel methods. The rate of these hydroxyl-related peaks does not relate impurities in the spinel structure but rather confirms surface intake phenomena, which can improve ability of spread out and may precipitated catalytic or surface binding properties of manganese ferrites nanoparticles.

FTIR spectrum of pure manganese ferrites nanoparticles showing features functional groups and metal–oxygen bonds. As shown in figure 3, peaks outcomes study.

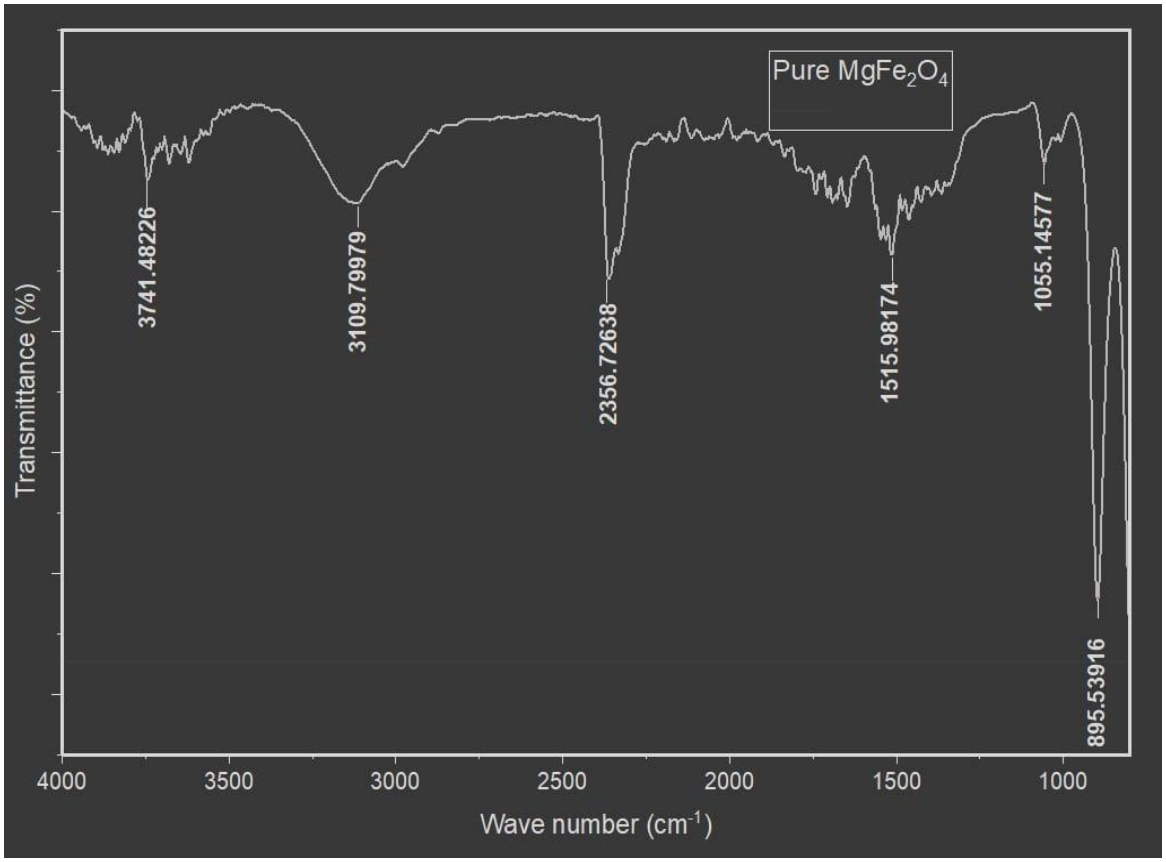

Figure 3: FTIR spectrum of pure manganese ferrites.

A different intake peak is noted at about 2356 cm^{-1}, typically related with the irregular secured shaking of atmospheric carbon dioxide (CO_2). This band commonly occurs in FTIR readings and extends from CO_2 present in the atmospheric environment during analysis. Another necessary band shows up at 1516 cm^{-1}, which can be generated on bending shaking of attached water molecules (H–O–H bending mode) or

unused nitrate groups if nitrate salts were used as metal precursors. In some cases, this area may also show small signs of organic remains from synthesis tuner or fuel agents. However, the relatively low size of this band points that any remaining pollutants are remaining, testing strong heating and phase formation. The lack of strong peaks matching to C–H pulling vibrations (around 2850–2950 cm^{-1}) shows that organic former was successfully extracted during thermal treatment, verifying the formation of a quite total oxide phase.

A moderate-intensity band at nearby 1055 cm^{-1} can be offered to C–O stretching vibrations or Fe–O–H bending vibrations. In ferrite systems, this region rarely copies remaining carbonate species formed due to climatic CO_2 link with surface metal ions. The quite weak size shows only surface-level surface capture other than mass combination. Another visible peak is located at 895 cm^{-1}, important because it lies within the lower frequency region connected with metal–oxygen distended vibrations in spinel ferrites. In $MgFe_2O_4$, the spinel structure contains of Mg^{2+} and Fe^{3+} ions divided between tetrahedral (A) and octahedral (B) sites within an oxygen lattice. Typically, tetrahedral (A-site) metal–oxygen vibrations appear around 550–600 cm^{-1}, and octahedral (B-site) metal–oxygen vibrations appear around 400–450 cm^{-1}. Although the spectrum extends only down to approximately 900 cm^{-1}, the incidence of the 895 cm^{-1} band indicates the onset of metal–oxygen lattice vibrations. The fundamental Fe–O and Mg–O stretching modes usually occur below 600 cm^{-1}, which may not be fully visible in the current spectral range. Contrarily, the low-wavenumber absorption confirms the formation of the spinel ferrite network.

The most pivotal finding for $MgFe_2O_4$ formation in FTIR analysis lies in the metal–oxygen long vibrations. In spinel ferrites, two principal absorption bands are compulsory: a higher frequency band shared to tetrahedral site vibration and a reduce frequency band corresponding to octahedral site vibration. Although the spectrum emphasizes higher wavenumber regions, the view of absorption below 1000 cm^{-1} verifies the presence of metal–oxygen bonds characteristic of ferrites. The deficiency of strong impurity peaks, such as unreacted Fe_2O_3 or MgO, further verifies phase purity. In addition, the relatively sharp and clear absorption features show excellent and successful crystal structure formation of $MgFe_2O_4$ nanoparticles, a peak broader could promote amorphous characteristics. As shown in table 1, the peaks overview.

Table 1. FTIR sample peaks position and their corresponding wavelengths.

Wavenumber (cm^{-1})	**Observed Peak**	**Functional Group**	**Comments**
3741	Weak	Free –OH stretching	Indicates adsorbed moisture or surface hydroxyl groups, typical for nanoparticles
3109	Broad	Hydrogen-bonded O–H stretching	Suggests physically adsorbed water or residual hydroxyl groups; broadness indicates H-bonding

Wavenumber (cm^{-1})	Observed Peak	Functional Group	Comments
2356	Distinct	Asymmetric stretching of CO_2	Arises from atmospheric CO_2; not part of ferrite structure
1516	Medium	H–O–H bending / residual nitrate groups	Low intensity suggests minimal residual impurities; confirms effective calcination
1055	Medium	C–O stretching / Fe–O–H bending	May indicate surface carbonate species; weak intensity implies surface adsorption only
895	Noticeable	Onset of metal–oxygen (M–O) lattice vibrations	Confirms formation of spinel ferrite network; fundamental Fe–O and Mg–O vibrations occur below 600 cm^{-1}

Conclusion

The FTIR spectrum showed evidence for pure $MgFe_2O_4$ nanoparticles offers clear absorption peaks that give definition into the chemical bonding and the physical model of the material. The broad band attained around 3109 cm^{-1} is pointing of O–H stretching vibrations, which are limits of surface-adsorbed hydroxyl groups or moisture present in the sample. Such signals are common in ferrite nanoparticles due to their peak surface area and the occurrence of naturally used water molecules. The peak near 2356 cm^{-1} likely link to CO_2 arriving at modes, which may derive from climatic air or trace carbonate chemical form that were not fully deleted during the synthesis process. Another key peak found at 1515 cm^{-1} can be given to arching vibrations of O–H bonds, showing the presence of hydroxyl groups or maybe organic spare from starter used during the synthesis. Critically, the area between 1055 cm^{-1} and 895 cm^{-1} shows strong intake bands, which are traits of metal–oxygen (M–O) waves in the dorsal structure. Principally, the bands near 1055 cm^{-1} can be joined with the expanding vibrations of Mg–O bonds at the four-sided sites, while the band about 895 cm^{-1} relations to Fe–O stretching in the eight-faced sites. These M–O vibrations verify the formation of the dorsal ferrite structure and point out optimal blend of magnesium and iron ions into their specific lattice places. Additionally, the drain of a small band at 3741 cm^{-1} may show detail surface binding sites or remaining functional groups that did not contain in the lattice formation but remain on the nanoparticle surface, which can apply properties such as water affinity and adsorption conduct. Overall, the FTIR spectrum gives a complete knowledge of both the layer chemistry and the inner bonding of $MgFe_2O_4$ nanoparticles, verify that the merged material shows the likely spinel ferrite characteristics while also protection surface features that may damage its chemical response and boundary with external molecules. These seen align with past summaries on magnesium ferrite nanoparticles, marking characteristic M–O vibrational modes in the lower wavenumber zone and surface hydroxyl removal at higher wavenumbers, certify that the synthesis method used is intense in compiling pure, crystalline spinel ferrite nanoparticles fit for further networks in catalysis, magnetic devices, or external upgrades.

References

1. Hulla, J.E., S.C. Sahu, and A.W. Hayes, Nanotechnology: History and future. Human & experimental toxicology, 2015. 34(12): p. 1318-1321.

2. Bhushan, B., Introduction to nanotechnology: history, status, and importance of nanoscience and nanotechnology education, in Global perspectives of nanoscience and engineering education. 2016, Springer. p. 1-31.

3. Ganji, D.D. and S.H.H. Kachapi, Introduction to nanotechnology, nano mechanics, micromechanics, and nanofluid. Application of nonlinear systems in nano mechanics and nanofluids, 2015.

4. Choudhary, F., et al., A review on synthesis, properties and prospective applications of carbon nanomaterials. Nano-Structures & Nano-Objects, 2024. 38: p. 101186.

5. Abegunde, S.M., M.O. Alaka, and O.I. Awonyemi, Nanomaterial toxicity: A comprehensive review of mechanisms and mitigation strategies. Discover Hazards, 2025. 1(1): p. 1-19.

6. Joudeh, N. and D. Linke, Nanoparticle classification, physicochemical properties, characterization, and applications: a comprehensive review for biologists. Journal of nanobiotechnology, 2022. 20(1): p. 262.

7. Barhoum, A., et al., Review on natural, incidental, bioinspired, and engineered nanomaterials: history, definitions, classifications, synthesis, properties, market, toxicities, risks, and regulations. Nanomaterials, 2022. 12(2): p. 177.

8. Yuan, X., et al., Cellular toxicity and immunological effects of carbon-based nanomaterials. Particle and fiber toxicology, 2019. 16(1): p. 18.

9. Darwish, M.A., et al., Advancements in nanomaterials for nano sensors: a comprehensive review. Nanoscale Advances, 2024. 6(16): p. 4015-4046.

10. Cullity, B.D. and C.D. Graham, Introduction to magnetic materials. 2011: John Wiley & Sons.

11. Heck, C., Magnetic materials and their applications. 2013: Elsevier.

12. White, R.M., Quantum theory of magnetism: magnetic properties of materials. 2007: Springer.

13. Krishnan, K.M., Fundamentals and applications of magnetic materials. 2016: Oxford University Press.

14. Fiorillo, F., Characterization and measurement of magnetic materials. 2004: Academic Press.

15. Rao, B.S., et al., Preparation and characterization of CdS nanoparticles by chemical co-precipitation technique. Chalcogenide Lett, 2011. 8(3): p. 177-185.

16. Sharma, R., et al., X-ray diffraction: a powerful method of characterizing nanomaterials. Recent research in science and technology, 2012. 4(8).

17. Ai, A., UV-Vis Spectroscopy–Principle, Instrumentation, Applications, Advantages, and Limitation.

18. Al-Amin, K., et al., Fourier transform infrared spectroscopic technique for analysis of inorganic materials: a review. Nanoscale Advances, 2025. 7(21): p. 6677-6702